Exploration Geophysics, Remote Sensing and Environment XXX.2 (2023)

DOI: 10.26345/EGRSE-044-23-204

A CASE STUDY OF THE GROUND-PENETRATING RADAR METHOD IN THE DIAGNOSIS OF THE TECHNICAL CONDITION OF THE KOŠICE BRIDGE

PRÍPADOVÁ ŠTÚDIA VYUŽITIA GPR PRI DIAGNOSTIKE TECHNICKÉHO STAVU MOSTA V KOŠICIACH

René Putiška[1], Bibiana Brixová[1], Eduard Vyskoč, Martin Bednarik[1], Vladimír Budinský[2], Marta Prekopová[3]

Abstract

The aim of this study is to present, on a particular example, the possibilities of using georadar measurements in the diagnostic assessment of a bridge structure. Ground-Penetrating Radar (GPR) measurements provide valuable information in diagnostic assessments, which is why they were included among the non-destructive methods in the diagnostics of the technical condition of the bridge with an underpass in Košice (Slovakia). GPR measurements with antennas with frequencies of 450 MHz and 750 MHz provided the data covering the thickness of the asphalt layer in the part of the bridge top, captured the effects of the steel reinforcement and the decline of the reinforced concrete structure caused by the deformation of the bridge cover. Based on the attenuation of the signal on some radargrams, which indicates an increased humidity of the environment, sections with a presumed damage to the waterproofing of the bridge were determined. Measurements with a high-frequency antenna (2000 MHz) on the lower structure of the bridge (underpass) captured the changing thickness of the cover layer of the steel reinforcement and confirmed the fault in waterproofing in certain sections. As part of the comprehensive diagnostics, the compressive strength of concrete was also determined by a non-destructive method (Schmidt's hammer), detection of interfaces with increased humidity by capacitive humidity measurement, measurement of chloride content in the surface concrete layer, detection of the condition of subsurface expansion joints and assessment of the condition of the track bed. The data from these measurements and observations supplemented and confirmed the results of the GPR measurement. The radargrams and their interpretation thus provided sufficient information about the state of the cover layer of the steel reinforcement and the state of the waterproofing, necessary for the resolution of the renovation of the object, so that the planned inspection boreholes, which would only worsen the state of the waterproofing, did not need to be realised.

Abstrakt

Cieľom tejto štúdie je prezentovať, na konkrétnom príklade, možnosti využitia georadarových meraní pri diagnostickom posudku stavebnej konštrukcie. GPR merania poskytujú pri diagnostických posudkoch cenné informácie, preto boli začlenené medzi nedeštruktívne metódy i v rámci diagnostiky technického stavu mosta s podchodom v Košiciach (Slovensko). GPR merania s anténami o frekvenciách 450 MHz a 750 MHz nám v časti mostového zvršku poskytli údaje o hrúbke asfaltovej vrstvy, zachytili prejavy oceľovej výstuže a pokles železobetónovej konštrukcie spôsobenej deformáciou mostného uzáveru. Na základe útlmu signálu na niektorých radargramoch, ktorý indikuje zvýšenú vlhkosť prostredia, boli určené úseky s predpokladaným narušením hydroizolácie mosta. Merania vysokofrekvenčnou anténou (2000 MHz) na spodnej stavbe mosta (podjazd) zachytili meniacu sa hrúbku krycej vrstvy výstuže a potvrdili porušenia hydroizolácie v určitých úsekoch. V rámci komplexnej diagnostiky bolo realizované aj zisťovanie pevnosti betónu v tlaku nedeštruktívnou metódou (Schmidtovo kladivo), zisťovanie rozhraní so zvýšenou vlhkosťou kapacitným meraním vlhkosti, meranie obsahu chloridov v povrchovej betónovej vrstve, zistenie stavu podpovrchových mostných uzáverov a posúdenie stavu koľajového lôžka. Údaje z týchto meraní a pozorovaní doplnili a potvrdili výsledky GPR merania. Radargramy a ich interpretácia tak poskytli dostatočné informácie o stave krycej vrstvy oceľovej výstuže a stave hydroizolácie, potrebné pre riešenie sanácie objektu, takže plánované vývrty, ktoré by stav hydroizolácie iba zhoršili, nebolo treba realizovať.

Keywords

Ground-Penetrating Radar, geotechnical survey, diagnostics of bridge structures, concrete moisture determination, Schmidt hammer

Kľúčové slová

GPR, geotechnický prieskum, diagnostika stavebných konštrukcií, stanovenie vlhkosti betónu, Schmidtovo kladivo

1. Introduction

This paper presents the possibility of using Ground-Penetrating Radar (GPR) measurements in the evaluation of the existing bridge structure and is aimed at inspection of the current state of the bridge body, the state of remodelling and assessing the state of the structure itself and the properties of building materials. Projects focused on the diagnosis of the technical condition of structures (e.g. bridge structures) within the framework of improving the quality of diagnostics open up possibilities for the use of geophysical methods mainly due to their non-destructive approach and the continuous information they provide. GPR measurements are a frequently used geophysical method.

GPR enables to obtain precise information about structures below the surface and at different scales, for example, directly in geology when exploring the subsoil (Al-Shukri et al., 2014; Busby et al., 2004) and groundwater resources (Paz et al., 2017), but also in archaeology (Basile et al., 2000; Yousef et al., 2020) and also when solving engineering geological tasks dealing with e.g. stability of slopes (Xie et al, 2018; Pupatenko et al., 2019; Bednarczyk, 2016). GPR measurements have found great application in the field of geotechnical exploration

Fig. 1 The diagnosed object - a bridge with underpass to the ZŤS (VSS) in Košice

(Lanbo and Xiongyao 2013; Quinta-Fereira 2019; Lai et al., 2017; Shaaban and Al-Salami, 2014), road construction and concrete structures. Within the scope of geotechnical and engineering tasks, the most common goal is to verify the feasibility of reconstruction or to extend the life of the structure, to check the reliability and to determine the rate of deterioration. Such non-destructive methods help in diagnosis to determine the desired properties without extensive damage to the building material or structural element. However, their interpretation requires advanced engineering knowledge and basic physical and chemical knowledge to avoid incorrect assessments.

GPR measurements were also included in the comprehensive diagnostics of the technical condition of the bridge with an underpass in Košice (South-East of Slovakia). The diagnosed object is a bridge - underpass (Fig. 1). The self-diagnosis concerned the bridge deck, supporting structure, substructure (underpass) consisting of supports, pillars and wings, as well as sidewalks and railings. The main goal of the GPR measurements was to determine the thickness of structural layers and the state of waterproofing and to determine the thickness of the cover layer of the reinforcement. In addition, the compressive strength of concrete was determined by a non-destructive method (Schmidt's hammer), detection of interfaces with increased moisture by capacitive measurement of moisture and detection of seepage through waterproofing, measurement of the chloride content in the concrete surface layer of the concrete parapet, mapping of cracks and irregularities, detection of the condition of subsurface expansion joints and assessment of the condition of the track bed.

The diagnosis itself, and thus the GPR measurement within the lower part of the structure, was complicated by the presence of about 80 cm of water in the entire section of the underpass.

2. Measurement methodology

Ground-Penetrating Radar

Ground-Penetrating Radar (GPR), also known as georadar, is a method using radar pulses to map structures and objects below the surface. Transmitted electromagnetic waves pass through the environment, while the enveloping curve of electromagnetic waves has the shape of a cone expanding towards the depth. When a wave hits the interface of layers that have different dielectric parameters, part of the energy is reflected, and the rest continues to propagate in the medium. The energy of the reflected wave is recorded and displayed in the form of a timeseries, where the amplitudes and time of passage through the individual layers can be seen. Based on the parameters of recorded reflected waves (size and frequency, time shift between their sending and receiving), information about the state of the diagnosed environment is obtained.

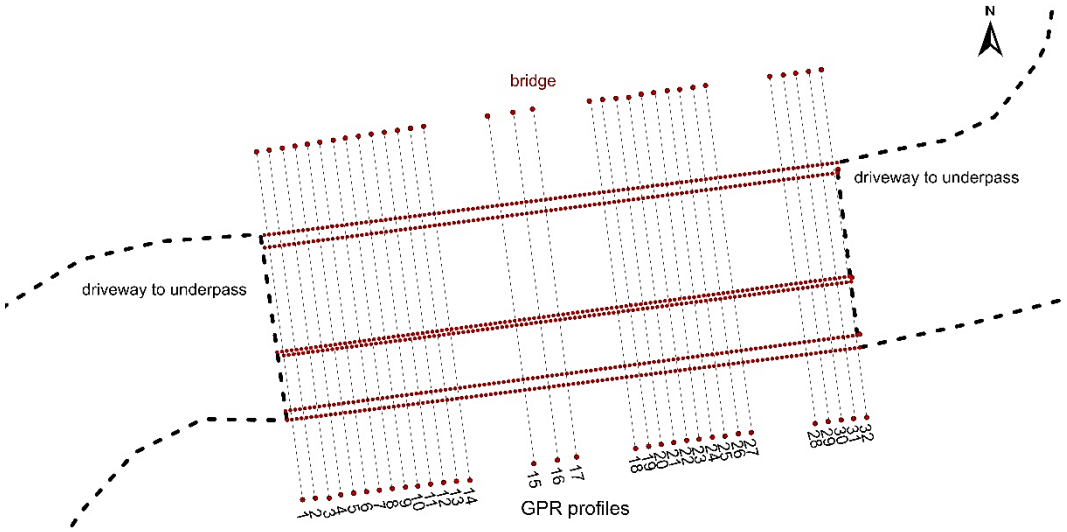

Fig. 2 Distribution of GPR measurement profiles on the bridge top

To determine the thickness of the road layers and the condition of the waterproofing on the bridge deck, the Ground Explorer georadar from Mala with HDR technology and GX450MHz and GX750MHz antennas were used. The antenna with a lower frequency and a deeper range was used to diagnose deeper structural layers and detect faults in the concrete lintel of the bridge, whereas the antenna with a higher frequency and finer resolution was utilised for detailed mapping of road layers and the state of waterproofing. GPR was applied to 32 measuring profiles (1-32) oriented perpendicular to the bridge (Fig. 2). The measurements were carried out in position and height with Trimble GeoXR equipment using GNSS technology (RTK method using the SKPOS service). The altitude of the points was determined in the binding Bpv system.

A Palm 2000 MHz antenna from GSSI was used to detect the cover layer of reinforcement within the substructure. The positioning of the georadar profiles is shown in Fig. 3. One longitudinal profile P1 with a length of 42 m and 17 short transverse profiles P2 to P18 were implemented on the inner wall of the underpass (Fig. 3). One longitudinal profile P22 with a length of 47 m and 6 short transverse profiles P24 to P29 were implemented on the outer wall of the underpass. One P23 profile was located on the ceiling of the underpass.

Capacitive humidity measurement

The detection of interfaces with increased moisture (capacitive measurement of moisture) was realized with the MERLIN EVO cc (concrete construction) device, which is intended for measuring the water content in plaster and concrete. A capacitor formed by a spring

Fig. 3 The location of the profiles when measuring the structural elements of the substructure (underpass) with the GPR antenna 2000 MHz

contact is placed on the construction sample. An alternating electric field that, depending on the shape, penetrates the sample to a greater or lesser depth (Fig. 4). The depth of penetration of the electric field of the capacitor into the measured material is between 2 and 5 cm. This depends on the shape and structure of the layer. The water contained in the building material has a substantial effect on the electric field. The changes in the field are therefore evaluated as water content.

Fig. 4 Measuring device MERLIN EVO cc and the principle of capacitive humidity measurement

The device was set to measure the mass moisture content of concrete (measurement range from 0.2% to 5.0%). It calculates the water content in weight percent of the total weight of building materials (dry) without destruction and displays the moisture as the weight of water in % weight (weight of water relative to the weight of the dry sample).

The measurements themselves were carried out on four profiles under the bridge (inside the underpass). The measurement locations are shown in Fig. 3.

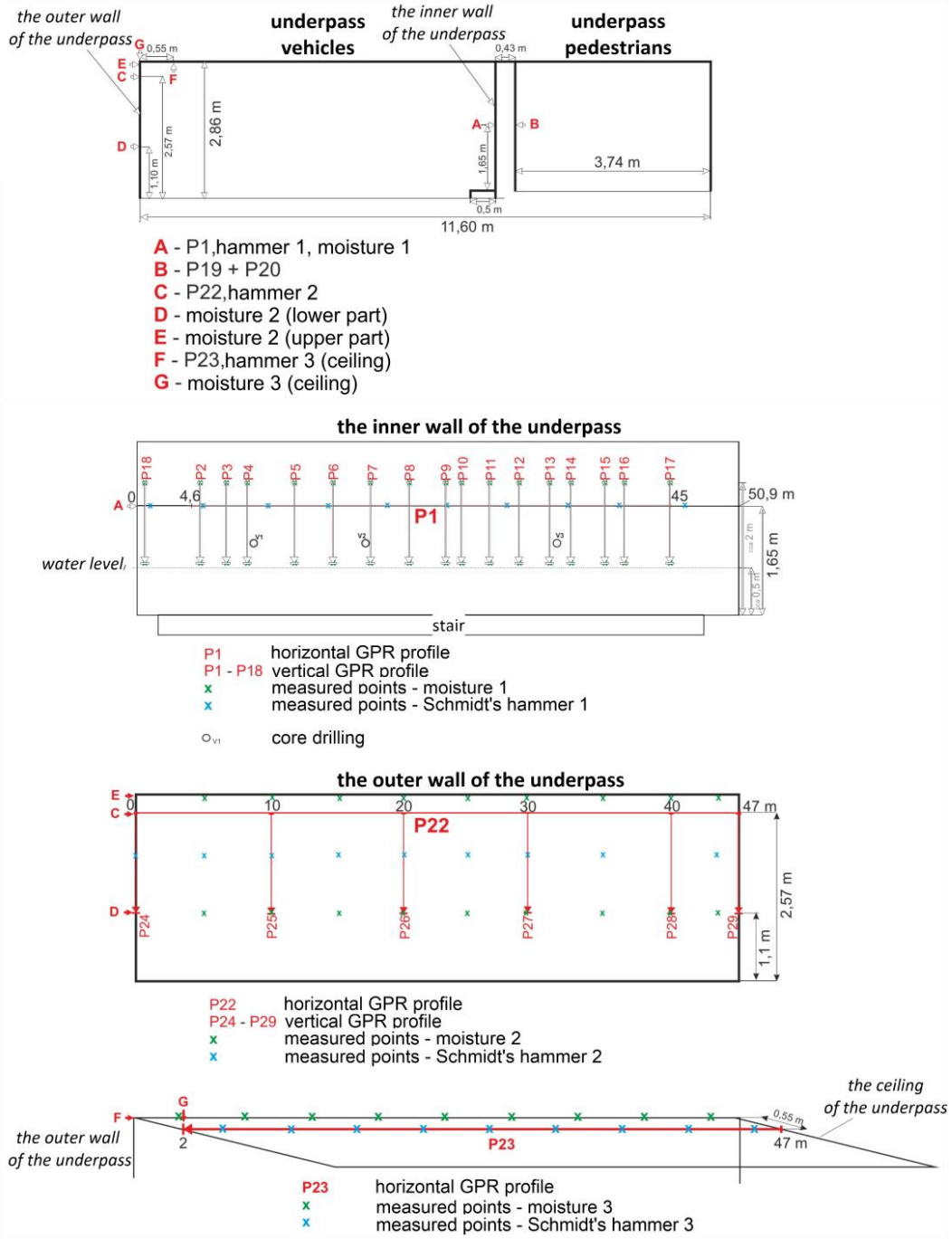

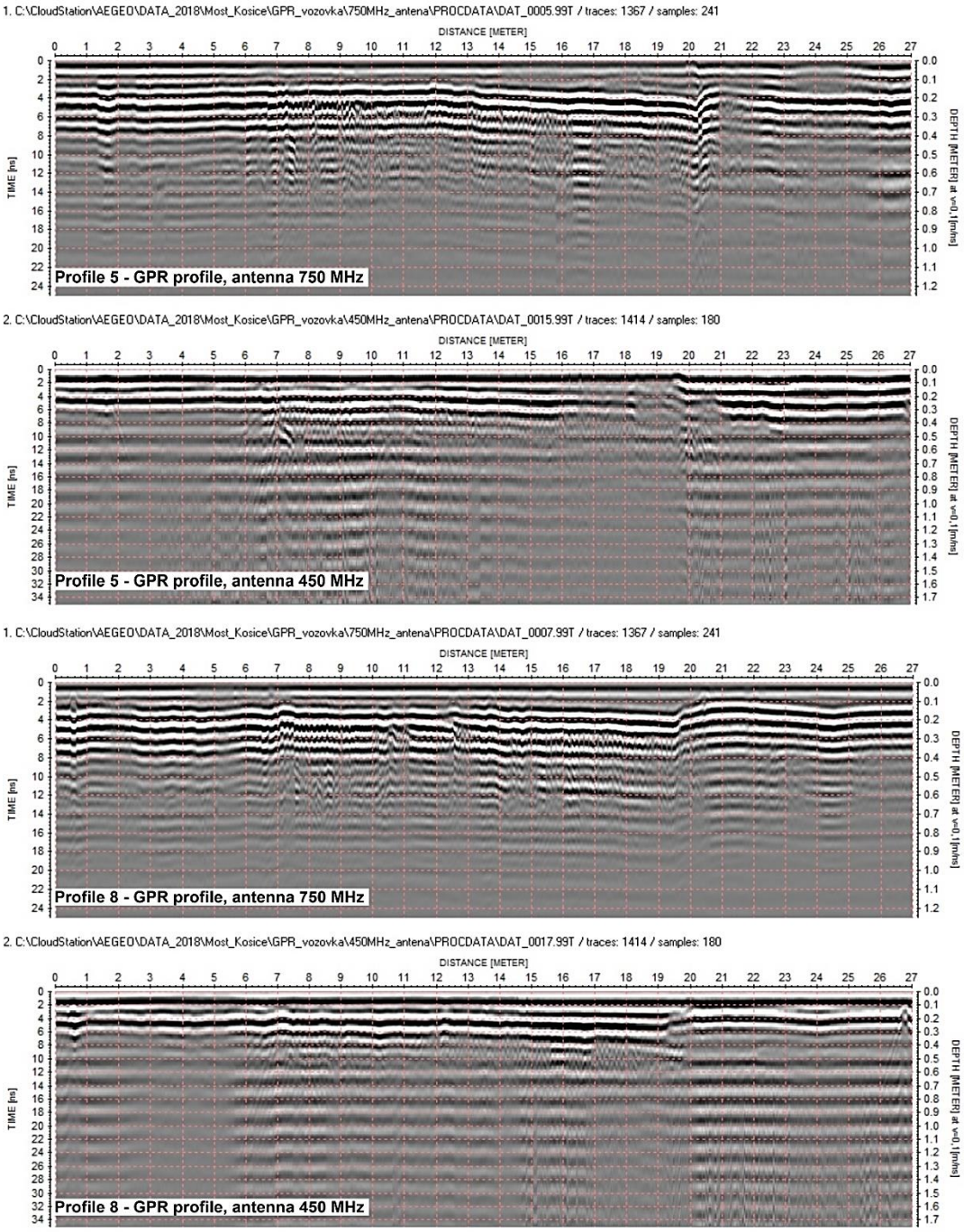

Fig. 5 Radargram on profile 5 and 8 – bridge top, road section. Effects of the steel reinforcement are visible in the distance 6.5 – 20 m. Drop of the reinforced concrete structure due to the deformation of the bridge cap is observed in the depth 25 - 35 cm.

Determining the compressive strength of concrete (Schmidt's hammer)

A non-destructive test of the compressive strength of concrete (according to STN 73 1373) of the reinforced concrete supporting structure of the bridge was performed on the vertical surface of the wall from the side (horizontally, at each measured point one measurement) and on the ceiling of the underpass vertically upwards (at each measured point one measurement). A total of 30 measurements were taken, 10 vertically upwards, 20 horizontally (10 outer wall, 10 inner wall of the underpass).

Measurement of chloride content in the surface concrete layer of a concrete parapet

To determine the chloride content in concrete, four concrete samples were taken from the concrete parapets and walls of public transport shelters. The buildings were extremely damaged by concrete corrosion with exposed and corroded reinforcement. The samples taken were analysed in the testing laboratory of the Technical Testing Institute of Construction in Bratislava.

3. Measurement results

Ground-Penetrating Radar

Bridge deck

The results of georadar measurement on the bridge deck yielded information about the thickness of the asphalt layer, which ranges from 15 to 20 cm on profiles 5 to 19 (Fig.5). On profiles 18 to 27, the thickness of the asphalt is about 25 cm. On profiles 1 to 4, which are located on the sidewalk, the asphalt reaches a thickness of approx. 20 cm. Under the layer of asphalt, the reinforced concrete construction of the bridge begins. On profile 5 (Fig. 5) there is a nicely captured steel reinforcement at the 6.5 and 20.5 meters, which is located at a depth of 25 cm at the 6.5 m meter and progresses to a depth of 35 cm, which it reaches at the 20 m meter. This shift is probably caused by the deformation of the expansion joints. A very similar decrease of the reinforced concrete structure is also captured on radargrams from profiles 5 to 11 (Fig. 5). Prominent horizontal interfaces appeared on profiles 12, 13 and 14, as well as attenuation in the deeper parts of the radargram, which probably indicates increased moisture in the structural layers. The increased humidity of the structural layers in the form of signal attenuation in the deeper parts of the profile was also manifested on the opposite side of the road on profiles 18 to 27. The steel reinforcement is visible on these profiles at a depth of 40 cm, i.e. in a lower position than on the other side of the road.

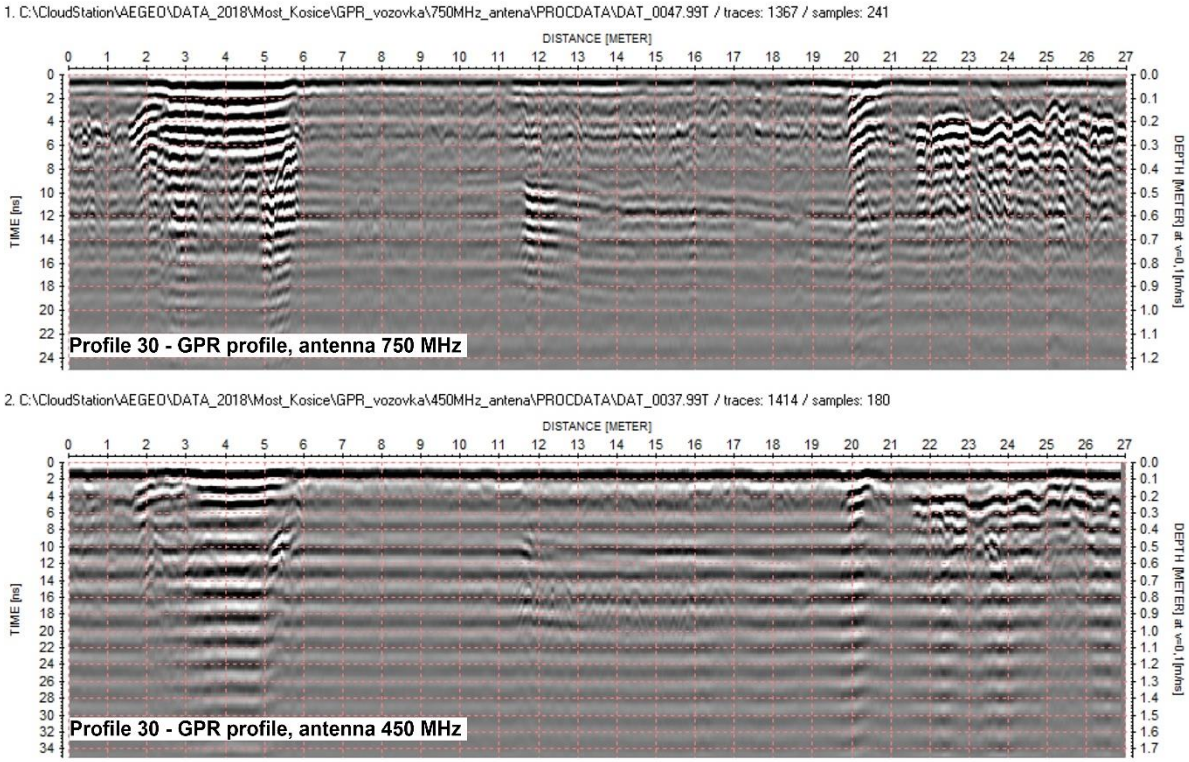

Fig. 6 Radargram on profile 30 – bridge top, footpath section. Attenuation of the signal in deeper parts caused by moisture indicates the damage of the waterproofing. The beginning and the end of the bridging, effects of the steel reinforcement are visible at a depth of approx. 70 cm.

Profiles 1 to 4 and 28 to 32 are located on sidewalks (see Fig. 2). On profiles 28 to 32, there is considerable signal attenuation over the entire section of the bridge structure (distance 5.5 to 20 m). In this section, significant damage to the waterproofing is expected, which resulted in wetting of the structural layers of the bridge. The beginning and end of the bridge can be seen on the

radargrams, and on the sections from 12 to 16 m there are signs of steel reinforcement at a depth of 70 cm (Fig. 6). In the case of profiles 1 to 4, the expansion joints are located at 5.6 m and 20.8 m, but the information about the bridging is obscured by parallel utility networks.

Profiles 15 to 17 are located directly on the tram line leading over the bridge. The reinforced concrete structure is located in this section at a depth of approx. 20 cm. The thickness cannot be determined from the results, as the dense steel reinforcement does not allow the analysis of deeper structures (Fig. 7).

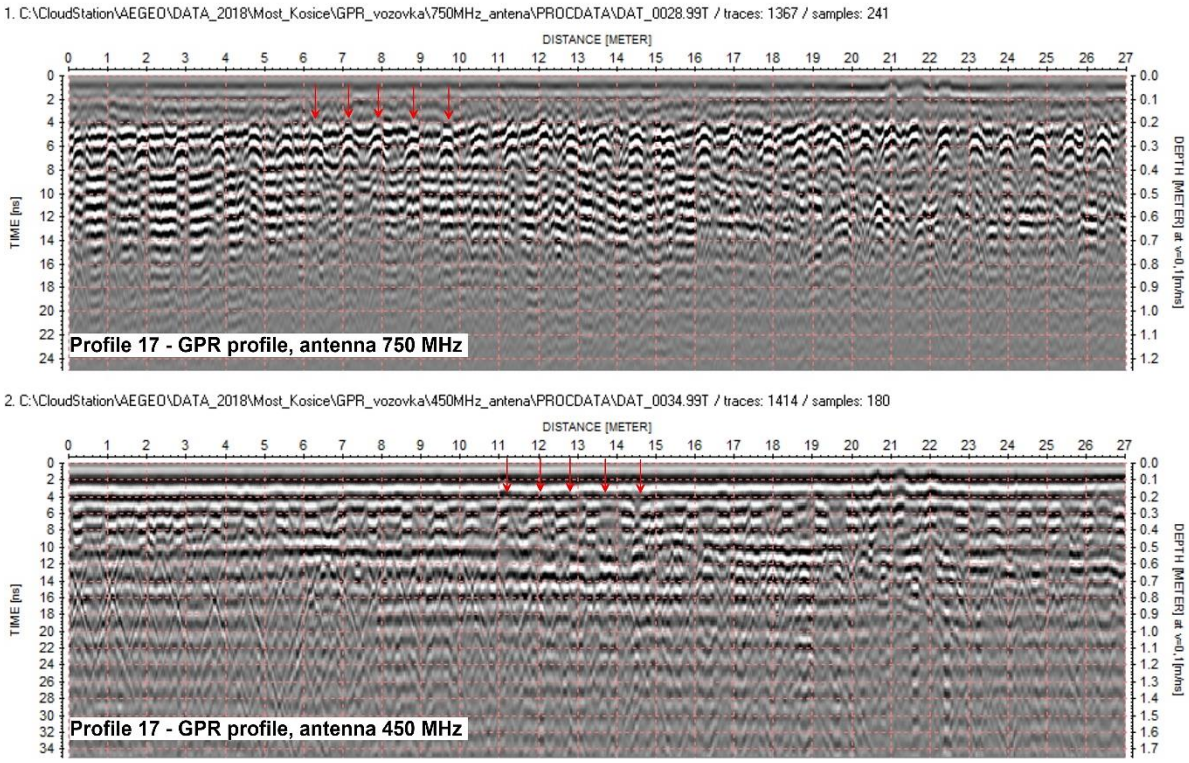

Fig. 7 Radargram on profile 17 – bridge top, tram track section. The dense steel reinforcement prevents from the analysis of deeper structures. The red arrows indicate some examples of steel reinforcement manifestation.

Underpass construction

During measurements with a high-frequency antenna on the lower structure representing the supports, pillars and wings of the underpass, a covering layer of reinforcement with a thickness of 15 mm to 45 mm was detected on the longitudinal profile P1 on the inner wall of the underpass (see Fig. 3). The steel reinforcement is approximately every 20 cm in this direction (Fig. 8). Measurements on the transverse profiles P2 to P18 show that the cover layer of the reinforcement also moves in the transverse direction in the interval from 25 to 45 mm, and the individual bars of the reinforcement are also separated by approx. 20 cm (Fig. 9). The red line in the radargrams determines the thickness of the cover layer and the depth of the reinforcement.

The measurement results on the longitudinal profile P22 on the outer wall of the underpass (see Fig. 3) show that the covering layer of the reinforcement is about 45 mm thick for the first 7 m, then the thickness gradually decreases up to a length of 19 m where it slowly disappears (Fig. 10). In these places, the steel reinforcement comes to the surface or is located very close to the surface, up to a height of 43 m. The decrease of the cover layer towards the inside of the tunnel is also documented by transverse profiles. The cover layer of reinforcement on profile P24 is approx. 27 mm (Fig. 11a), on profile P25 approx. 18 mm (Fig. 11b) and absent on profiles P26, P27 and P28 (Fig. 11c) and on profile P29 its thickness is approx. 16 mm (Fig. 11d).

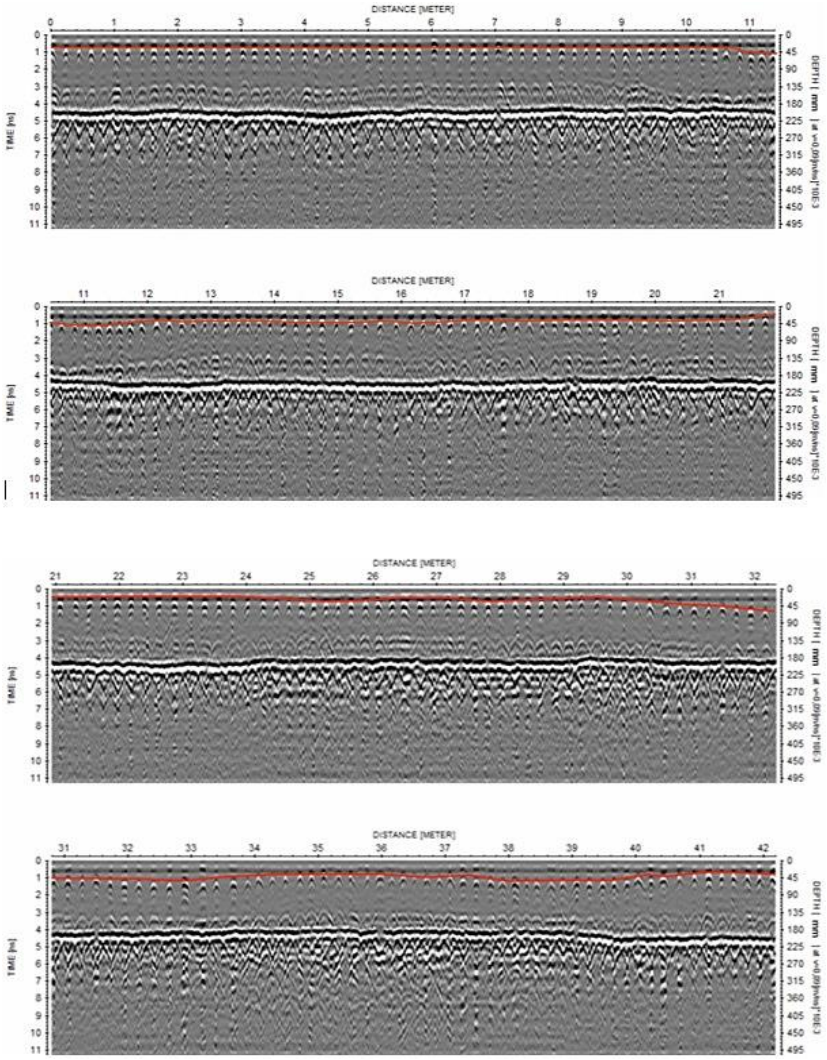

Fig. 8 Radargram on profile P1 – inner wall of the underpass, longitudinal profile. The presence of steel reinforcement is visible in an interval of approx. 20 cm, and the thickness of the covering layer of reinforcement is 15-45 mm. The red line indicates the depth of the steel reinforcement.

Based on the radargram, the thickness of the cover layer of the reinforcement was determined to be approximately 18 mm on the profile P23 along the underpass ceiling (see Fig. 3). The steel beams appeared as a prominent reflector approx. every 35 cm (Fig. 12). The radargram also shows a strong attenuation of the signal caused by the increased humidity of the material, on the basis of which it is assumed that the waterproofing is leaking.

Capacitive humidity measurement

The measurements were processed into illustrative graphs in which the higher value represents a greater amount of water (Fig. 13).

The results of the capacitive measurement of humidity show that the concrete structure is significantly soaked in water. The inner wall absorbs water mainly in the lower part, the construction of which is below the water level. This fact is also proven in Fig. 14a, where the humidity increases from the ceiling downwards. The situation is different on the outer wall of the underpass, which absorbs water from the lower - flooded part of the underpass,

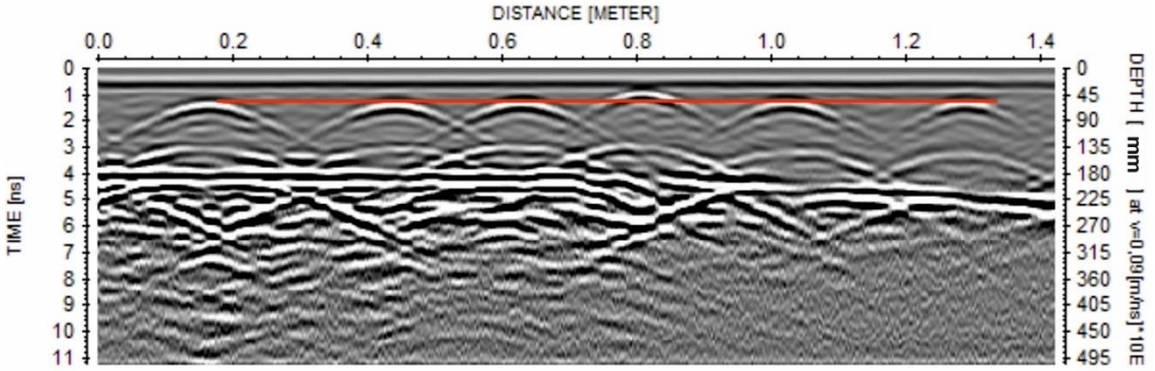

Fig. 9 Radargram on profile P3 – inner wall of the underpass, transverse profile. The appearance of the steel reinforcement is in an interval of approx. 20 cm, the thickness of the cover layer of the reinforcement in the transverse direction is 25 - 45 mm. The red line indicates the depth of the reinforcement.

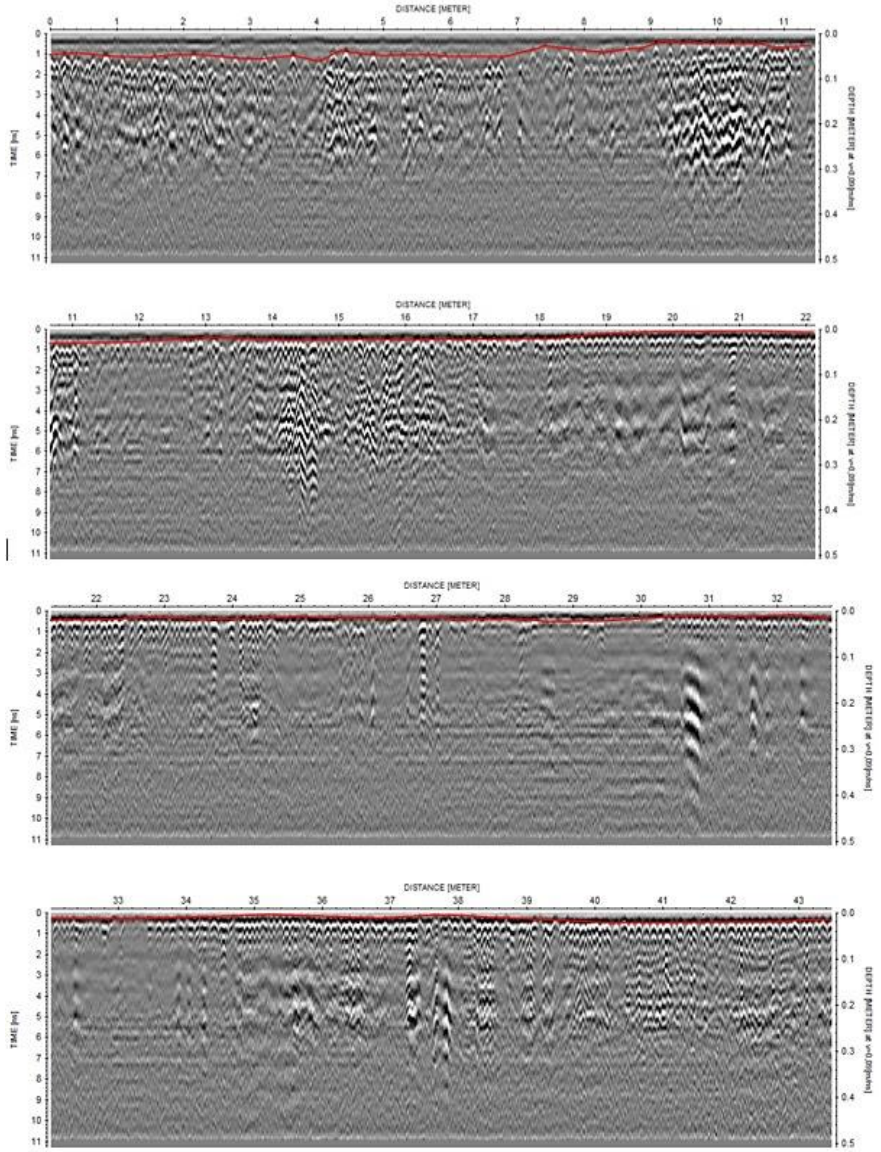

Fig. 10 Radargram on profile P22 – outer wall of the underpass, longitudinal profile. Decreasing of the covering layer towards the inside of the underpass. In the section 19 m – 43 m, the absence of a covering layer. The red line indicates the depth of the reinforcement.

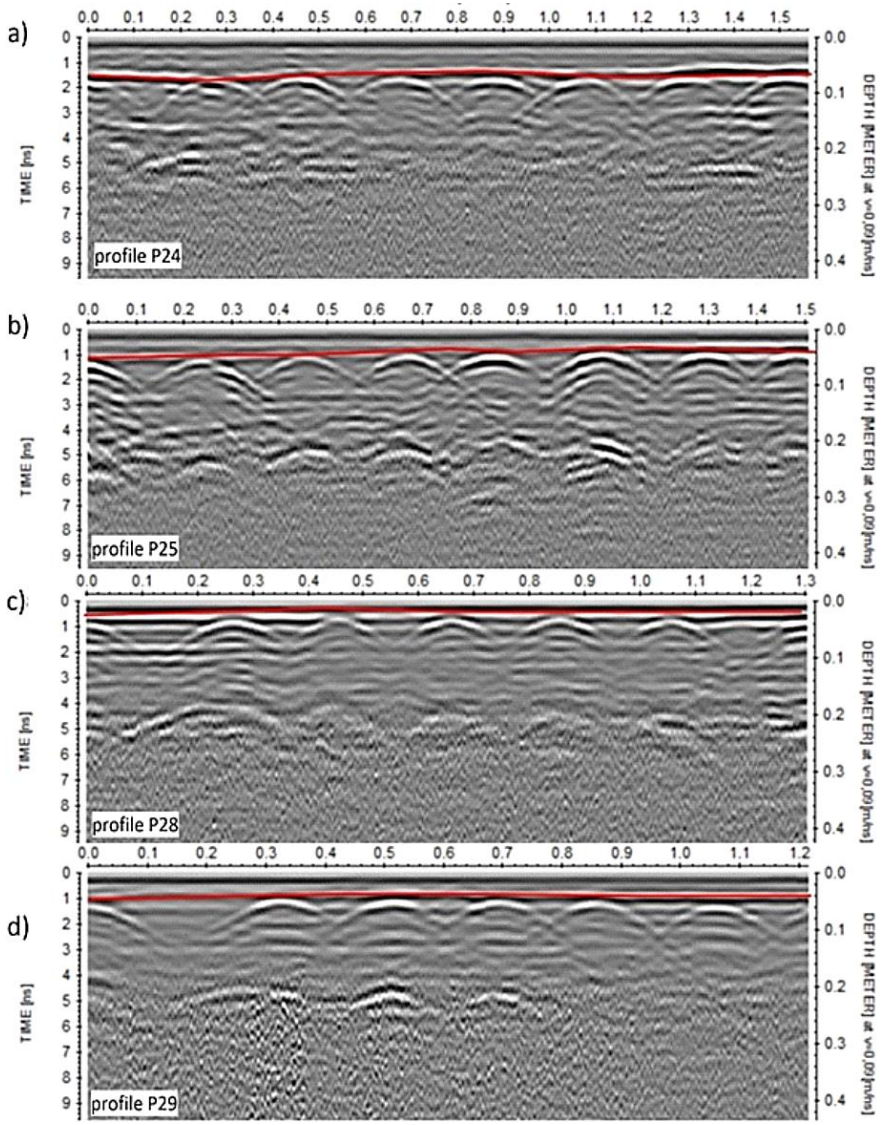

Fig. 11 Radargram on profile P24 (a), P25 (b), P28 (c) and P29 (d) – outer wall of the underpass, transverse profiles. Decrease of the cover layer of the reinforcement towards the inside of the tunnel. The red line indicates the depth of the reinforcement.

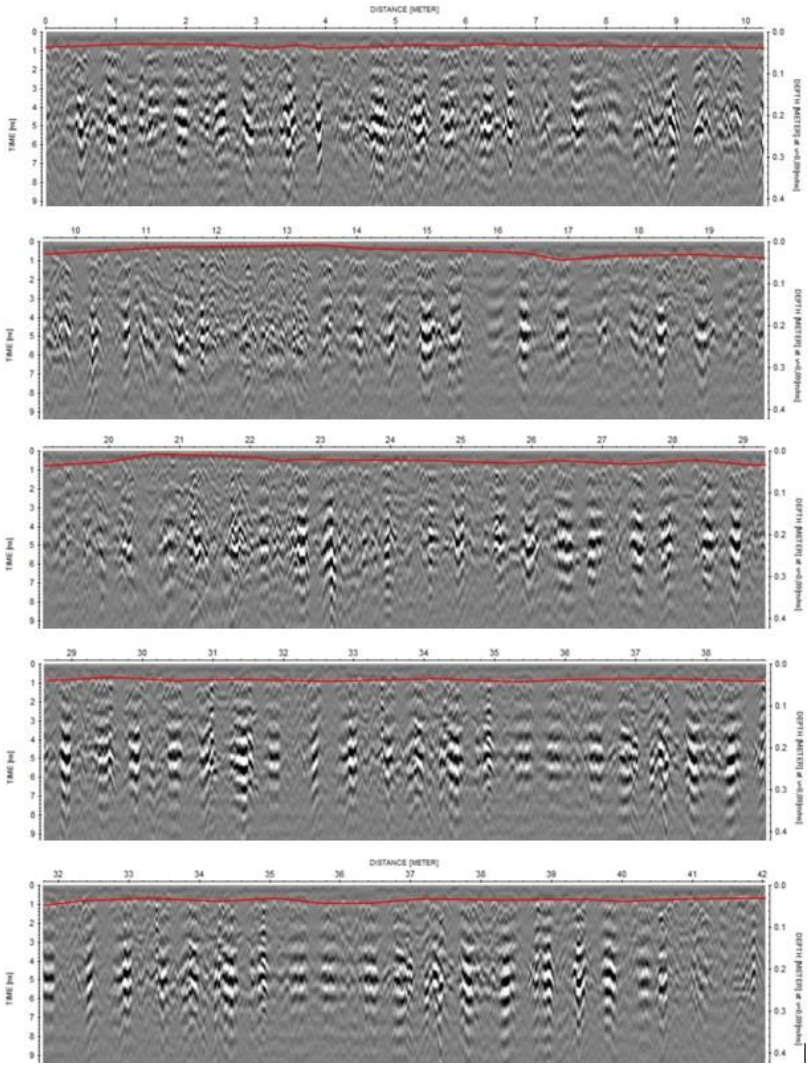

Fig. 12 Radargram on P23 profile – underpass ceiling, longitudinal profile. The appearance of the steel reinforcement in an interval of approx. 35 cm, the thickness of the cover layer of the reinforcement in the longitudinal direction is approx. 18 mm. The red line indicates the depth of the reinforcement. Attenuation of the signal in deeper parts caused by moisture indicates damage to the waterproofing.

but also from the upper part, through damaged waterproofing, mainly in places of expansion joints. This fact is documented by the following photo shown in Fig. 14b.

The ceiling of the underpass as well as the outer wall of the underpass have extremely high humidity in the second part of the profile starting at 25 m, which fits very well with the georadar results - profiles 18 to 27. In this part, we expect significant damage to the waterproofing and expansion joints.

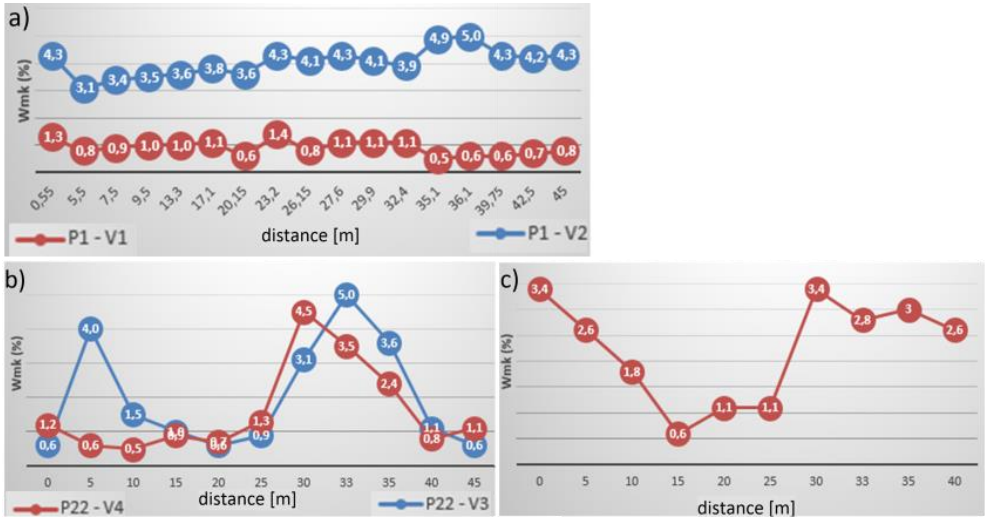

Fig. 13 Results of capacitive humidity measurement

a) Internal wall of the underpass. V1 – measurement in the lower part of the wall (110 cm above the road), V2 – measurement in the upper part of the wall (200 cm above the road)

b) The outer wall of the underpass. V3 – measurement in the lower part of the wall (110 cm above the road), V4 – measurement in the upper part of the wall (200 cm above the road)

c) Underpass ceiling

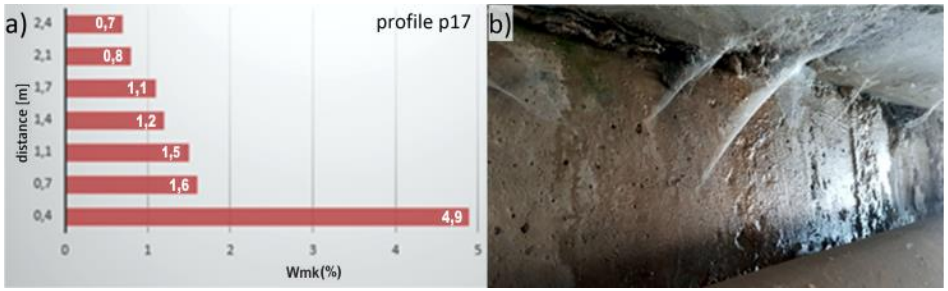

Fig. 14 a) Vertical profile of the humidity change - inner wall of the underpass

b) photo - leaks through waterproofing

Fig. 15 Failure of the track bed

Determining the condition of subsurface bridge expansion joints

Based on the georadar measurement results shown in Fig. 5 to 12 and capacitive moisture measurement, we can state that georadar profiles 5 to 14 are about 10 cm higher than profiles 18 to 27, on georadar profiles 5 to 14 there is a drop of the reinforced concrete structure to the north (toward the outer wall of the underpass) and georadar profiles 18 to 27 have significant signal attenuation caused by higher humidity. The ceiling of the underpass as well as the outer wall of the underpass have extremely high humidity in the second part of the profile from the distance of 25 m (below georadar profiles 18 to 27).

The condition of subsurface expansion joints is evident from the presented results of georadar measurement and capacitive moisture measurement. Due to the evidently reconstructed road surface, the differences are currently not visible on the outside, except for the significantly high humidity of the underpass wall.

Assessment of the condition of the track bed

The track bed is placed in a U-shaped reinforced concrete structure. The bed itself is (based on the visible aggregate grains) of relatively large fractions (approx. 63 mm), without significant content of smaller filling grains. The surface of the track bed is covered with a layer of asphalt concrete.

The problematic place of the track bed is the place where the tracks lead above the edge of the bridge from the city side - it is evident that the bed itself just next to the edge has settled and the tracks are partially in the air (Fig. 15) - the visible bends of the track have disturbed the asphalt concrete cover of the bed in the area of the tracks and the bends of the tracks when passing trams are visible to the naked eye (range approx. 1 - 2 cm).

Tab. 1 Measurement results with Schmidt hammer type NR with recording device, 1 - 10 internal wall of the underpass, 11 - 20 external wall of the underpass, 21 - 30 ceiling

Measured point	Measured values	Value of $R_{be}´$ [MPa]	Compressive strength of concrete with not guaranteed accuracy $R_{be} = \alpha_t . \alpha_w . R_{be}´$ [MPa]
1	46	52	46,8
2	43	46	41,4
3	39	39	35,1
4	41	42	37,8
5	41	42	37,8
6	40	41	36,9
7	45	50	45,0
8	33	28	25,2
9	33	28	25,2
10	41	42	37,8
11	44	48	43,2
12	40	41	36,9
13	39	39	35,1
14	42	44	39,6
15	23	<16	values below the lower range limit
16	8	<16	values below the lower range limit
17	30	24	21,6
18	25	16	14,4
19	29	22	19,8
20	37	35	31,5
21	54	60	54,0
22	58	62	55,8
23	53	58	52,2
24	48	49	44,1
25	37	28	25,2
26	44	41	36,9
27	22	<14	values below the lower range limit
28	57	62	55,8
29	22	<14	values below the lower range limit
30	27	<14	values below the lower range limit

Determining the compressive strength of concrete by a non-destructive method (Schmidt's hammer)

The evaluation of the concrete compressive strength test (according to STN 73 1373) of the reinforced concrete supporting structure of the bridge is in Tab. 1. During the evaluation, the articles 35 and 36 of STN 73 1373 regarding the age and moisture content of the concrete (values $\alpha_t = 0.90$ and $\alpha_w = 1.00$) were taken into account.

Based on the determined values of the compressive strength of concrete (with accuracy not guaranteed), the concrete of the inner wall construction can be considered as concrete of strength class C16/20 to C20/25, whereas the concrete of the outer wall and partly of the ceiling construction cannot even be considered as concrete of strength class C16/20.

Measurement of chloride content in the surface concrete layer of a concrete parapet

The result of the chemical analysis of the cement taken from the parapets and walls of the public transport shelters are the chloride contents in the individual samples listed in Tab. 2. The permitted content of chlorides in

reinforced concrete (0.4%) was slightly exceeded in only one sample, the other two samples had a significantly smaller content.

Tab. 2 Chloride content in samples from the surface concrete layer of the concrete parapet

Sample No.	Measured Values (% mass)		
	Individual values		Average value
1	0,078	0,078	0,078
2	0,019	0,018	0,019
3	0,032	0,032	0,032
4	0,443	0,443	0,443

4. Conclusion

Ground-Penetrating Radar (GPR) measurements on the diagnosed bridge in Košice brought valuable information about its condition. In the lower part of the bridge (on the inner wall, the outer wall, and the ceiling of the underpass), the measurements brought information about the thickness of the cover layer of the reinforcement and the depth of the reinforcement under the surface. The results show that mainly the outer retaining wall of the underpass is in poor condition. The radargrams show the loss of the cover layer towards the inside of the underpass, where the cover layer of the reinforcement is absent or only very thin and the steel reinforcement here shows a high degree of corrosion. The measurements also confirmed the leakage of the waterproofing in the underpass ceiling.

On the section of the bridge top, based on GPR measurements, the thickness of the asphalt and the condition of the structural layers were determined, and damage to the waterproofing was confirmed, mainly in the north-east part of the structure and the places of the bridge expansion joints. The results were so convincing that the inspection core drilling that was planned as part of the bridge diagnostics did not have to be carried out. The resulting holes would only result in further damage to the waterproofing.

The results of GPR measurements provided continuous information along the entire length of the measured profiles. They thus made it possible to continuously monitor changes in the properties of the diagnosed materials without destructive interventions and thus contribute to the design of a solution for the object's rehabilitation. And that is the task of applied geophysics - to provide a continuous picture of the distribution of physical properties of materials under the surface and thus contribute to refinement of solutions in other disciplines.

Acknowledgement

This work was supported by research projects APVV-16-0146, APVV-19-0150 and VEGA 1/0107/23.

References

AL-SHUKRI, H., MAHDI, HANAN., AL KADI, O. Application of ground penetrating radar for near surface geology. 2014, https://www.researchgate.net/publication/266047479_APPLICATION_OF_GROUND_PENETRATING_RADAR_FOR_NEAR_SURFACE_GEOLOGY

BASILE, V., CARROZZO, M.T., NEGRI, S., NUZZO, L., QUARTA, T., VILLANI, A.V. A ground-penetrating radar survey for archeological investigations in an urban area (Lesse, Italy). *Journal of Applied Geophysics 44*, 2000, 15-32.

BEDNARCZYK, Z. Near-surface geophysical scanning for examplar landslide projects in Poland. Geotechnical and Geophysical Site Characterisation 5 – Lehane, acosta-Martinez&Kelly, Sydney, Australia, Australian Geomechanics Society, 2016 https://www.issmge.org/uploads/publications/25/26/ISC5_118.pdf

BUSBY, J. B., CUSS, R. J., RAINES, M. G., BEAMISH, D. Application of ground penetrating radar to geological investigations. Brithish Geological Survey, Internal report IR/04/21, 2004, http://nora.nerc.ac.uk/id/eprint/11336/1/IR04021.pdf

LAI, W.L.W., DÉROBERT, X., ANNAN, P. A review of ground penetrating radar application in civil engineering: a 30-year journey from locating and testing to imaging and diagnosis. *NDT and E international, p.2, Elsevier,* 2017.

LANBO, L., XIONGYAO, X., GPR for geotechnical engineering. *Journal of Geophysics and Engineering*, 2013, Vol. 10, n. 3.

PAZD, C., ALCALÁ, F. J., CARVALHO, J. M., RIBEIRO, L., Current uses of ground penetrating radar in groundwater-dependent ecosystems research. *Science of The Total Environment,* 2017, Vol. 595, p. 868-885.

PUPATENKO, V., SUKHOBOK, Y., STOYANOVICH, G., STETSYUK, A., VERKHOVTSEV, L., GPR data interpretation in the landslides and subgrade slope surveys. *MATEC Web of Conferences 265*, 03003, GCCET, 2019, https://doi.org/10.1051/matecconf/201926503003

QUINTA-FERREIRA, M., Ground Penetration Radar in Geotechnics. Advantages and Limitations. *IOP Conference Series: Earth and Environmental Science, Vol. 221*; World Multidisciplinary Earth Sciences Symposium 2018, Prague, Czech Republic, 2019.

SHAABAN, F., AL-SALAMI, A.E., Geotechnical studies for evaluation and limitations of environmental and engineering hazards that affect the economic infrastructure in Abha, Saudi Arabia. *NRIAG Journal of Astronomy and Geophysics*, 2014, Vol. 3, Issue 2, p. 150-162.

XIE, P., WEN, H., XIAO, P. Evaluation of ground-penetrating radar (GPR) and geology survey for slope stability study in mantled karst region. *Environ Earth Sci 77*, 2018, 122. https://doi.org/10.1007/s12665-018-7306-9

YOUSEF, S.B.A., YOUSEF, M.H.M., ABD-ELSALAM, H.F., SHAHEEN, M.A.M. Detection of the Possible Buried Archeological Targets using the Geophysical Methods of Ground Penetrating Radar (GPR) and Self Potential (SP), Kom Ombo Temple, Aswan, Governorate, Egypt. Geomaterials, 2020, Vol. 10, No. 04, 105-117.

Authors:

[1]Department of Engineering Geology, Hydrogeology and Applied Geophysics, Faculty of Natural Sciences, Comenius University in Bratislava, Ilkovičova 6, 842 15 Bratislava, Slovakia

[2]Institute of Geosciences, Faculty of Mining, Ecology, Process Control and Geotechnologies, Technical University of Košice, Letná 9, 040 01 Košice, Slovakia

[3]ekolive s.r.o., Americká Trieda 2430/3, Košice, Slovakia